

# Antennas design and distribution for a LOFAR Super Station in Nançay

J. N. Girard\*, P. Zarka\*, M. Tagger†, L. Denis‡, D. Charrier§, A. Konovalenko¶

## Abstract

The Nançay radioastronomy observatory and associated laboratories are developing the concept of a “Super Station” for extending the LOFAR station now installed and operational in Nançay. The LOFAR Super Station (LSS) will increase the number of high sensitivity long baselines, provide short baselines and an alternate core, and be a large standalone instrument. It will operate in the low frequency band of LOFAR (30–80 MHz) and extend this range to lower frequencies. Three key developments for the LSS are described here: (i) the design of a specific elementary antenna, and the distribution of such antennas (ii) at small-scale (analog-phased mini array) and (iii) at large-scale (the whole LSS).

## 1 Introduction

The renewed international interest for low frequency radioastronomy has given birth to many ground-based projects. One of them is the dutch-european LOw Frequency ARray (LOFAR), working in the 30-250 MHz range. It is a very large radio interferometer composed of phased arrays of antennas (so-called “stations”) spread at up to 100 km from a central “core” in the Netherlands, with remote stations at up to  $\sim 1000$  km in nearby european countries (France, Germany, Sweden, UK, ...). Each LOFAR station actually consists of two phased arrays of 48 (NL) or 96 (European) antennas : the low band antennas array (LBA) below the FM band ( $\sim 30$ -80 MHz) and the high band antennas array (HBA) above it (110-250 MHz). Along with an electronic cabinet (digital control, command, and receivers), they form a LOFAR “station”. After digitization, spatial beamforming, and spectral channelization, the signals of all stations are sent though optical fiber link to the central correlator in Groningen. More details are given in (De Vos et al., 2000) and on *www.lofar.org*. The Nançay Radio Observatory (*www.obs - nançay.fr*) hosts the international station “FR606”.

---

\*LESIA - Observatoire de Paris, CNRS, Meudon, France

†LCP2E, Université d’Orléans, CNRS, Orléans, France

‡Station de Radioastronomie, Observatoire de Paris, CNRS, Nançay, France

§SUBATECH, Université de Nantes, France

¶Institute of Radio Astronomy, Kharkov, Ukraine

## 2 The LOFAR Super Station

### 2.1 Principle and general design

At any given time, a LOFAR station can use the LBA or the HBA field of antennas (not both) which are thus connected to two different inputs to the electronic cabinet. A third input to the cabinet's receivers exists, which was initially dedicated to a "Low Band Low" antenna field in the range 10-50 MHz, descoped for economic reasons in the course of the project. The main idea underlying the LSS concept is to build and connect to this input a new field of 96 antennas (the LSS field), operating in the LBA range and extending this range to lower frequencies (down to  $\leq 15$  MHz). Each of these new antennas will actually consist of an analog-phased mini-array of 10–20 antennas, increasing thus by a factor 10–20 $\times$  the sensitivity of the station in the LBA range, while remaining fully compatible with the whole LOFAR array (i.e. the LBA field still exists and is operational, and the signals from the LSS field can be correlated with LBA signals from the other LOFAR stations).

Each LSS mini-array of 10-20 antennas (dual-polarized) must be analog-phased because only 96 dual-polarization inputs to the cabinet's receivers are available. These mini-arrays are actually very similar in their principle to the HBA tiles of 16 (4 $\times$ 4 square grid) elementary high frequency antennas, thus we can also call them "LSS tiles". As HBA tiles, LSS tiles will consist of dual-polarized crossed dipoles, phased using delay lines (commutable cables lengths or any other frequency independent phasing system) so that their summed signals form a beam that can be pointed toward any direction of interest. The differences with HBA tiles include operation at lower frequencies (longer wavelengths) which implies larger antennas and a mini-array layout not necessarily square. It is signals beamformed at the tile level that are digitized and numerically combined in the cabinet's back-end, either in summation (phased array) or in correlation (interferometer) mode. The LSS will consist of 96 mini-arrays distributed within  $\sim 150$  m of the LOFAR station cabinet (see Figure 1 right). Its layout must then be optimized at two different scales : mini-array and full LSS.

### 2.2 Interests of the LOFAR Super Station

#### 2.2.1 *Within the LOFAR array*

The LSS will provide several improvements to the present LOFAR design and capabilities.

First, the 10 – 20 $\times$  improved sensitivity of the mini-array compared to a standard LBA antenna will correspondingly increase the sensitivity of all long baselines involving the LSS. At present, only a subset of 6 core stations called the "SuperTerp" can be phased as a single large station, and correlated to all other individual stations. The LSS will thus approximately double the number of long baselines with high sensitivity.

Second, only station-to-station correlations were planned in the initial LOFAR project, which implies in the LBA range a minimum baseline length of one LBA field diameter

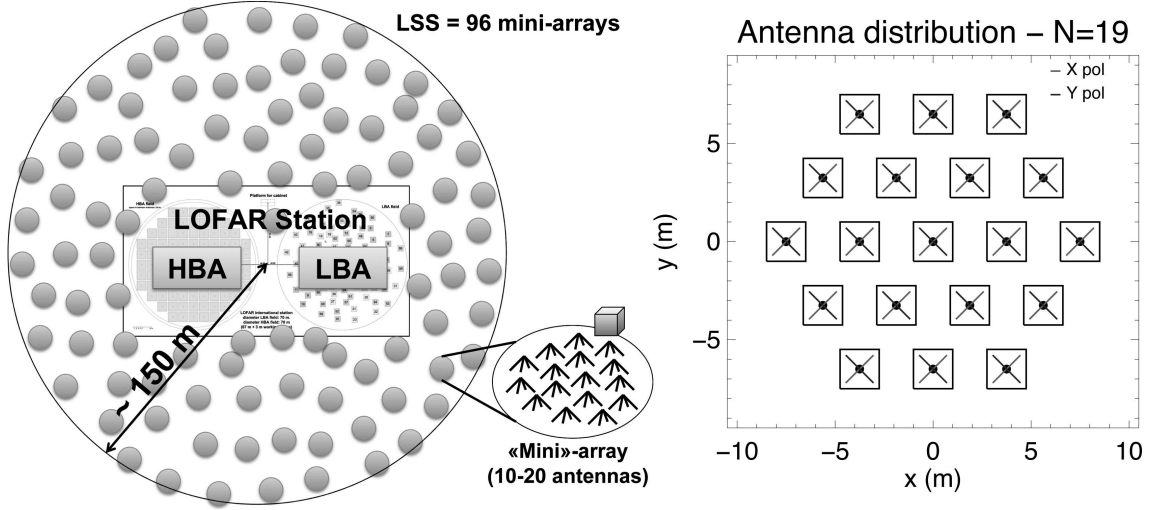


Figure 1: Left: The LOFAR Super Station is a set of 96 mini-arrays (or tiles) of 10-20 antennas analog-phased, spread around the Nançay international LOFAR Station within a range of  $\sim 150$  m. Right: Possible antennas distribution within a mini-array, here with  $N = 19$  elements arranged on an hexagonal grid. This distribution is a good compromise between an axisymmetric distributions (ensuring a low sidelobe level) and a regular array (providing easy analog phasing) (see 3.2).

( $B_{min} \sim 60$  m). This implies that LOFAR would be blind to structures larger than  $\lambda/B_{min}$  at wavelength  $\lambda$  (i.e. typically larger than a few degrees). In order to overcome this severe limitation to the imaging capabilities of LOFAR, it is planned to perform antenna-to-antenna correlations within LBA fields or within the SuperTerp, but the sensitivity of each individual LBA crossed dipole is very poor. With the LSS, tile-to-tile correlations will be performed, providing baselines as short as a mini-array diameter (10–15 m) and up to the LSS diameter ( $\sim 300$  m) with 10–20 times better sensitivity than antenna-to-antenna correlations. LSS will thus fill very efficiently a missing part of LOFAR’s present (u,v) coverage in the low band.

Third, several LOFAR observation programs (such as the “Epoch of Reionization” studies – [www.astro.rug.nl/~LofarEoR/](http://www.astro.rug.nl/~LofarEoR/)) will need large bandwidths and excellent calibration rather than high angular resolution and will consequently use only core stations (such use may represent  $\approx 30\%$  of the observation time). In the meantime, remote and international stations may be correlated in parallel by the central computer and run other programs, but these will not benefit of the core stations which bring an increased sensitivity and relatively short baselines. By correlating the LSS to all remote and international stations, sensitive long baselines will be restored. The LSS can thus be viewed as an alternate core (or a large SuperTerp), albeit not being placed at the center of the european LOFAR but rather at an edge. This inconvenient may be somewhat mitigated by reserving a few core stations for correlation with remote, international stations and the LSS, forming thus an interferometer with decent (u,v) coverage and good sensitivity, while using most of the core stations for the specific programs requiring only those. In this way, the LSS can contribute to “create” up to 30% of additional LOFAR observing time in parallel with

core-only observations.

### 2.2.2 As a stand-alone instrument

With  $N = 19$  antennas (Figure 1 right), the LSS will have an effective area  $\simeq 96 \times 19\lambda^2/4 \simeq 40000 \times (\lambda/10)^2$  comparable to that of the Giant Meterwave Radio Telescope (GMRT) in India,  $\simeq 3 \times$  the Very Large Array (VLA) in New-Mexico, or  $\simeq 10 \times$  the Nançay Decameter Array (NDA). It will thus be a large instrument by itself, with relevant standalone use independent of LOFAR, with no loss for LOFAR when the Nançay FR606 station is not included in ongoing observations (this should represent at least 10% of the time for international stations).

Moreover, the LSS elementary antennas can be designed in order to provide a better sensitivity and immunity to radio frequency interference (RFI) than LBA antennas, and to extend the spectral range of operation down to frequencies ( $< 30$  MHz).

### 2.2.3 Scientific objectives

Scientific programs of the LSS (within LOFAR or in standalone mode) will include low frequency surveys, detection of weak sources in time-frequency (coherent phased-array) mode, contribution to the study of large-scale diffuse structures, . . . and it will in addition provide a better calibration for VLBI imaging. A standalone LSS is also well adapted to student training purposes.

## 3 Three key design studies for the LSS

LSS feasibility, design, cost and prototyping studies are presently ongoing. We present below the results of three design studies that are crucial for the LSS: (i) the elementary antenna design, (ii) the antennas distribution in a mini-array, and (iii) the 96 mini-arrays distribution in the LSS.

### 3.1 Antenna design

Several low frequency ground-based instruments are presently under development : LOFAR, the Long Wavelength Array - LWA (Ellingson et al., 2009), the Murchison Widefield Array - MWA, the Giant Ukrainian Radio Telescope - GURT, . . . For each of them, specific elementary antennas have been developed in order to meet their scientific and technical requirements, as shown in Figure 2.

Antenna design implies the determination of physical (geometrical) and electrical parameters of the elementary antenna radiators (the receiving wires), which will in turn constrain the performances of the array in which they are grouped. These parameters are the antenna beaming pattern in E & H planes (constraining the array's Field of View - FoV),

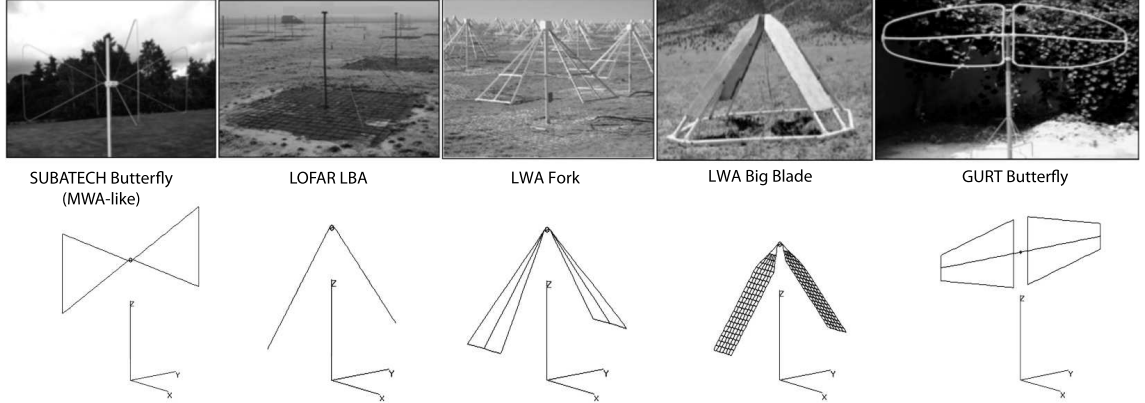


Figure 2: The top panel displays the linearly polarized dipoles that have been studied in Nançay. The bottom panel displays their numerical wire model as used in input of electromagnetic simulations with NEC – see text.

the level of side lobes (defining a Signal-to-Noise Ratio), the frequency bandwidth, and the efficiency (related to electrical and ground losses). At low frequencies, we work in a sky-dominated noise regime ( $T_{sky} \approx 60000K$  at 20 MHz) so that we can neglect the noise contribution from the antenna itself. In order to limit the noise of resistive parts of the instrument beyond the antennas (cables, electronics, ...), a low noise amplifier (LNA) is directly attached to the antenna radiators, forming a so-called “active” antenna.

For a phased-array application such as the LSS, with electronic pointing of the mini-arrays, a large and smooth beam pattern is required, close to that of an isotropic antenna, as it will condition the final FoV of the array, expected to go down to a elevation of  $20^\circ$  with LOFAR. Toward the horizon, extinction of the beam is preferred to reduce the susceptibility to RFI. We also wish to obtain a broadband antenna that can operate down to 15–20 MHz, implying an antenna input impedance ( $Z_{in} = R_{rad} + jX$ ) with radiation resistance  $R_{rad}$  and reactance  $X$  as constant as possible over the band of interest, with  $|X| \ll R_{rad}$ .

Cost effectiveness imposes to restrict to linearly polarized dipoles (circularly polarized antennas such as those of the NDA (Boischoot et al., 1980) are quite expensive). Thus we carried out comparative studies of the geometry of the radiators of the antennas of Figure 2 using the numerical electromagnetic code (NEC – [www.nec2.org](http://www.nec2.org)). This code, based on the method of moments, can derive among other relevant quantities the simulated far field pattern and the electrical parameters of any antenna defined by a wire model (see bottom of Figure 2) and feed (radiators are simulated in emission – characteristics in reception are obtained by application of the reciprocity theorem plus taking into account the matching of the radiator and the LNA). We investigated the two classes of radiator designs (“butterfly” or “bow-tie”, and “inverted-vee” antennas) and the influence of a ground plane (metal grid), and we performed optimization studies of their parameters (height, length, droop and fork angles, grid mesh size and step, ...).

These studies led us to select a “thick” (see Balanis, 2005) inverted-vee dipole similar to the LWA Fork, which revealed to be a good compromise between bandwidth, FoV

and gain. We found that - as for LOFAR and the LWA - a metallic ground screen is necessary for inverted-vee antennas in order to reduce ground losses (efficiency  $> 50\%$  - resp.  $> 80\%$  - of that of a Perfect Electrical Conductive plane at 20 MHz - resp. 80 MHz), and to ensure the stability of the antenna impedance against variations of the ground characteristics (dry or wet ground). In parallel, various LNA architectures and matching have been considered. A first prototype of this thick dipole has been built in Nançay in order to test the relevance of our simulation results against measurements on the sky.

### 3.2 Distribution of antennas within a mini-array

The role of the mini-array is to combine analog antenna signals to synthesize a single wide beam and coarsely point it toward the direction of interest. The fine pointing of the LSS beam resulting from the combination of the signals from the 96 mini-arrays will be performed by the LOFAR beamforming system in the station back-end, and the resulting LSS beam will be tapered by the beam pattern of the mini-array. The constraints on the distribution of the antennas within a mini-array include : a smooth primary beam width, with a low level of side lobes (high SNR), a large effective area (high sensitivity), a not too complex phasing scheme, a low mutual coupling between elementary antennas, ... These constraints are not independent. For example :

- a large effective area implies a large separation between antennas to minimize superposition of antennas' effective areas at low frequencies, and thus a low beamwidth and high side lobe level at higher frequencies;
- analog phasing of a regular mini-array is easier, but such an array has grating lobes as powerful as the main lobe that appear in the visible space for specific antenna spacings and pointing directions.

We first performed an optimization study of the mini-array distribution aiming at the maximum reduction of side lobes. We used global minimization algorithms such as the simulated annealing (Kirkpatrick et al., 1983) based on a thermodynamically-controlled Monte-carlo displacement of the positions of the antennas (prior to the final antenna design - see 3.1 - the elementary antenna beam pattern was approximated by a simple  $\cos^2$  of the zenith angle). The resulting distributions are dense arrays (whose compacity is limited by a threshold distance between antennas) displaying circular symmetries around the phase center but without any kind of periodicity (the array does not superimpose to itself after rotation of any angle  $\neq 2\pi$ ). Such an axisymmetric and aperiodic shape guarantees the minimization of the side lobes (down to -30 dB attenuation or more) and the absence of strong grating lobes. But it is also very difficult and costly to phase by analog means in practice, because the absence of regularity imposes one delay line per antenna.

Thus, we opted for an array of antennas presenting regularities along two orthogonal  $x$  and  $y$  directions (as in NDA or GURT), while being as close as possible to the optimized symmetric solutions found above. Regularities along  $x$  and  $y$  directions allow us to decompose the phase scheme in two successive steps (e.g. phasing of antenna lines along  $x$  followed by phasing of rows along  $y$ ). This implies large savings in cable lengths : phasing

of  $P$  lines of  $Q$  antennas only requires  $P * E(Q/2) + E(P/2)$  (where  $E(x)$  is the integer part of  $x$ ) delay lines by using smart combinations of pairs of antennas symmetrical relative to the center of each line on a single delay line. A good compromise between beam characteristics and phasing complexity is shown in Figure 1. By using a triangular lattice, it is possible to find a balance between periodicity (which causes large grating lobes but cheaper phasing) and axisymmetry (which reduces side lobes and give an axisymmetric primary beam).

Regular arrays also present the advantage to reduce the problems caused by mutual coupling between antennas, because all embedded antennas (i.e. not at the edges of the mini-array) behave in a similar way. Conversely, in irregular/aperiodic arrays, the coupling may vary substantially from one antenna to the next (especially near the antenna resonance frequency), modifying elementary antenna beam shapes, so that the synthesized mini-array beam may have a complex shape. Further studies of distribution, phasing, and coupling effects are ongoing.

### 3.3 Distribution of mini-arrays within the LSS

The LSS will consist of 96 mini-arrays distributed in an area of  $\sim 300$  m diameter around the back-end of the FR606 station. It will work either in a phased-array (also called “tied-array beam” or “single pixel”) mode, as any standard station, or in interferometer mode. The digitization of each mini-array output (beamformed) signal by the LOFAR station back-end gives a large flexibility in the distribution of the 96 mini-arrays. The final LSS response will result from the multiplication of the mini-array pattern with the pattern resulting from the distribution of the 96 mini-arrays. The main constraints that the LSS must fulfill are a low level of side lobes (in phased-array mode) and a good (u,v) coverage by the  $96 \times 95/2$  baselines (in interferometer mode). As the filling factor of a disk of 300 m diameter by mini-arrays of 19 antennas is high ( $\sim 64\%$  at 30 MHz), the LSS will be a rather dense array/interferometer at low frequencies. A pseudo-random homogeneous distribution of mini-arrays over the whole LSS area, taking into account specific constraints of the station environment (pond, building, other instruments ...) is an acceptable baseline solution. We are in the process of optimizing this first solution by using the algorithm described in (Boone, 2001). It is a “pressure-driven” algorithm that enables to optimize the (u,v) coverage (relative to a target (u,v) model) of a “gas” of individual antennas, taking into account an input “site mask”. Each antenna (here mini-array) is displaced iteratively along the mean pressure exerted on it that is computed from the distribution of visibilities involving this antenna.

Another major improvement of the LSS response is brought by rotating by a random angle each array relative to a reference direction (and rotating back the elementary antennas within the mini-array in order to keep all antennas along the 2 main polarization axes), as was done for the LOFAR antenna fields. We computed that this decreases by  $\sim 8$  dB the side lobes level. This rotation also modifies the mutual coupling between antennas within each mini-array (as the antennas are oriented differently relative to the mini-array layout). This situation may bring benefits to the LSS, but it will increase the complexity of its calibration. In preparation of this calibration, we are currently modelling the LSS

in interferometer mode using the MeqTrees software package (Noordam et al., 2010). It enables to establish the Measurement Equation describing the instrument and to solve it for its parameters (the so-called “Jones” matrices describing all effects affecting the signal path: gain variations, pointing errors, ionospheric effects, ...). MeqTrees allows to simulate the instrument response as well as to calibrate real data.

## 4 Conclusion

LSS detailed design, prototype and tests studies (including the construction of 3 mini-arrays), and cost evaluation, will be pursued in the next  $\sim 20$  months. Its detailed scientific case is being developed in parallel (and inputs are permanently welcome). We expect LSS construction to start in 2013. If the concept is successful, it could be applied by other european participants to LOFAR, preparing a future “super LOFAR”.

**Acknowledgements** : The authors acknowledge the support of the Observatoire de Paris, the CNRS/INSU, and the ANR (french “Agence Nationale de la Recherche”) via the program NT09-635931 “Study and Prototyping of a Super Station for LOFAR in Nançay”.

## References

- Balanis, C. A., Antenna Theory: Analysis and Design, 2nd. Ed., Wiley, 497-522, 2005.
- Boischot, A., C. Rosolen, M. G. Aubier, G. Daigne, F. Genova, Y. Leblanc, A. Lecacheux, J. de la Noë, and B. M. Pedersen, A New High Gain, Broadband Steerable, Array to Study Jovian Decametric Emission, *Icarus*, **43**, 399–407, 1980.
- Boone, F., Interferometric array design: Optimizing the locations of the antenna pads, *Astron. Astrophys.*, **377**, 368-376, 2001.
- De Vos, M., A. W. Gunst and R. Nijboer, The LOFAR Telescope: System Architecture and Signal Processing, *Proceedings of the IEEE*, **97**, 1431–1437, 2000.
- Ellingson, S. W., T. E. Clarke, A. Cohen, J. Craig, N. E. Kassim, Y. Pihlstrom, L. J. Rickard and G. B. Taylor, The Long Wavelength Array, *IEEE Proceedings*, **97**, 1421–1430, 2009.
- Kirkpatrick, S., C. D. Gelatt, and M. P. Vecchi M. P., Optimization by Simulated Annealing, *Science*, New Series **220** (4598), 671-680, 1983.
- Noordam, J. E., and O. M. Smirnov, The MeqTrees software system and its use for third-generation calibration of radio interferometers *Astron. Astrophys.*, **524**, A61, 2010.